FRACTURE CHARACTERIZATION OF EPOXY ADHESIVES USING PRE-CRACKED CT SAMPLES

M. Casasola[1], M.J. Lamela[1]*, A. Fernández-Canteli[1], Miguel Muñiz-Calvente[1], F. Pelayo[1], Adrián Álvarez-Vázquez[1], A. Salazar[2], J.M. Pintado[3]

[1]University of Oviedo, Gijón-Spain

[2]University Rey Juan Carlos, Móstoles-Spain

[3]Instituto Nacional Técnica Aeroespacial, Torrejón de Ardoz-Spain

Abstract

In this paper the critical stress intensity factor (K_{IC}) and the critical strain energy release rate (G_{IC}) were determined for the epoxy resin EPOLAM 2025 following the D5045 standard and using Compact Tension (CT) specimens. Given the difficulty to produce a pre-crack at the tip of the notch of the CT sample, that fulfils the standard requirements, alternative experimental methods were attempted. Furthermore, a finite element analysis using the commercial Abaqus code was carried out to obtain the fracture parameters numerically and to study the relationship between the crack length and K_I. Although the fracture parameters obtained experimentally are within the range of values expected for such a material, they may not be precise because of the inaccuracy of the pre-cracks. No alternative pre-cracking method was found to be more adequate than the one used in this work, but its efficiency could be proved numerically.

Keywords: *epoxy resin, fracture characterization, testing, numerical analysis*

I. INTRODUCTION

Industries such as the aeronautic, among others, require materials with high mechanical performance and also very good specific properties for the design of structural components. Therefore, the importance of the continuous research for new materials that provide, at least, an equivalent stiffness and strength as the currently used ones. [1]

The material being tested in this research project is an epoxy resin called EPOLAM 2025, which main use is as an adhesive joint and as the matrix in fibre reinforced plastics. To study its effectiveness, the material is characterised by the fracture parameters – critical stress intensity factor and critical strain energy release rate – using the ASTM D5045 standard. For that, the pre-cracking at the tip of the notch of the CT specimen is required. Due to the brittleness of the material, this is a difficult task and therefore, alternative methods are attempted. [2], [3]

The fracture parameters are, as well, obtained in the finite element Abaqus code, along with a study of the relationship between the crack length and the stress intensity factor and the verification of the effectiveness of a new method for pre-cracking.

II. METHODOLOGY

A. ASTM D5045 Standard [2]

The procedure for the characterization of CT samples made of plastic materials is explained in the ASTM D5045 standard. This characterization uses the critical stress intensity factor, $K_{IC,}$ and the critical strain energy release rate, $G_{IC,}$ at fracture initiation.

Some assumptions need to be considered. One of them is a linear elastic behaviour of the material, which is due to the relatively small size of the plastic region at the crack tip. Also, a state of plane strain at the crack tip due to the sharp crack under a tensile load is considered.

Two types of specimen need to be tested to compute the above-mentioned fracture parameters. For K_{IC}, it is only necessary the pre-cracked CT sample, but for G_{IC}, an indentation specimen is also needed. This indentation specimen will have the same dimensions as the CT sample, except for the notch, which is not included. Dimensions and shape of the specimens are shown in Fig. I, where B should be equal to the thickness of the sheet of material from which the specimens were obtained and the ratio W/B should be in the range 2 to 4.

The results of the fracture parameters depend on the testing speed and temperature.

Before carrying out the tests, it is needed to create a pre-crack at the tip of the notch, which will provide the minimal K_{IC}. Although different methods are suggested in the standard, it is recommended to be done by tapping a razor blade into the notch. Afterwards, the specimen can be tested by loading it in tension. In the case of the indentation samples, the test is performed directly without any pre-crack.

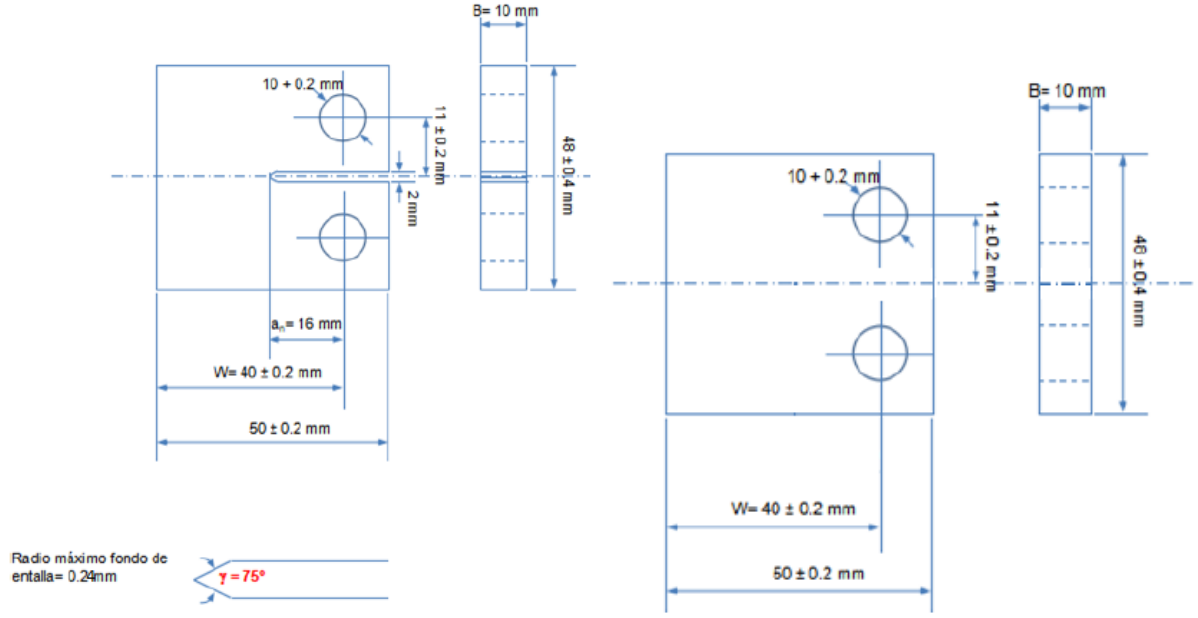

Fig. I. Dimensions of the CT specimen (above) and the indentation specimen (below).

B. Pre-cracking Methods

Effecting a sharp crack in a plastic material from a machined notch with considerable repeatable shape and size is difficult. It cannot be obtained by cyclic fatigue as in metals because, for brittle materials, there will be an unstable crack propagation.

Therefore, the standard specifies different methods. The most usual is to create the crack by tapping a razor blade into the notch. This method, besides providing a sharp crack, avoids plastic deformation and residual stresses in the area around the tip of the crack. If this method is not successful, it is also recommended to slide the razor blade in one motion or in a sawing motion into the notch, which minimizes the residual stresses in the region. [2]

As none of the explained procedures is highly accurate to produce a repeatability of the cracks, researchers from the University of Sheffield investigated about the matter and suggested an alternative method. This new method consists on simultaneously applying a compression load and a tensile load, in the vertical and transversal directions respectively, as shown in Fig. II. The tensile load will produce the crack while the compressive load will prevent it from growing. [3]

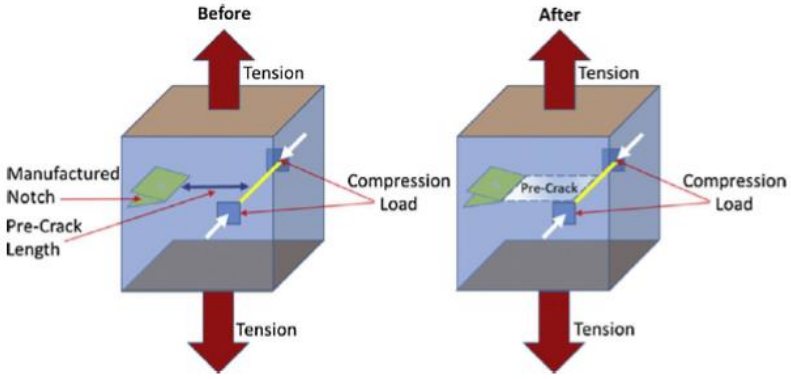

Fig. II. New method for pre-cacking.

The compression load is applied with a clamp that has got a rectangular contact area. To find the adequate forces to be applied, trial and error applies. Depending on the way the crack propagates, it is known which load to reduce or to increase to obtain the desired pre-crack, following the diagrams in Fig. III. If the compression load is too low, the crack will propagate through the specimen; if the compression load is too large, the crack will bifurcate; and if the crack is arrested at the desired point, the forces are adequate. [3]

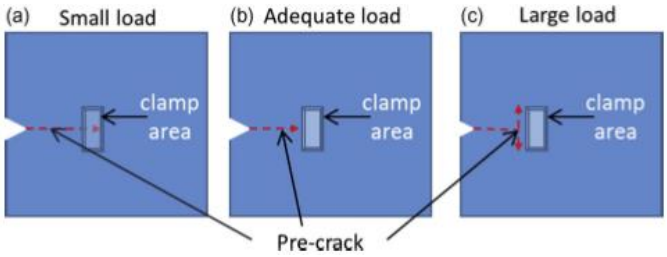

Fig. III. Growth of the pre-cracks depending on applied loads' value.

C. Abaqus

The finite element Abaqus code was used to perform a numerical analysis of the experimentally tested specimens. The fracture parameters were calculated, the relationship between the crack length and K_I was studied and the new pre-cracking method's effectiveness verified.

III. EXPERIMENTAL FRACTURE CHARACTERIZATION

The specimens used for the tests were made of EPOLAM 2025 and the manufacturing process was carried out by AXSON Technologies Spain, Instituto Nacional de Técnica Aeroespacial and Prodintec.

From a previous project, it is known that the ultimate tensile strength, σ_R, is 73 MPa and the Poisson ratio, ν, is 0.36. Young's modulus is believed to be around 2.2 GPa or around 3.2 GPa. [4]

For the pre-cracking three different methods were attempted. The one used for the first batch was tapping and it was performed on 13 specimens. 11 out of the 13 specimens were pre-cracked successfully, although the shapes and sizes were not repeatable nor adequate in all the cases. That was the reason to try other methods. The second batch's pre-cracks, which was formed by 3 samples, were attempted by fatigue. As expected, the method was not suitable. Finally, the third batch, which consisted on 6 specimens, was used to try the method developed by the researchers of the University of Sheffield. These results are explained in section III.C of this paper.

A. First Batch

The pre-cracked specimens were axially loaded in tension in an MTS device. From the output data, the graph in Fig. IV was obtained.

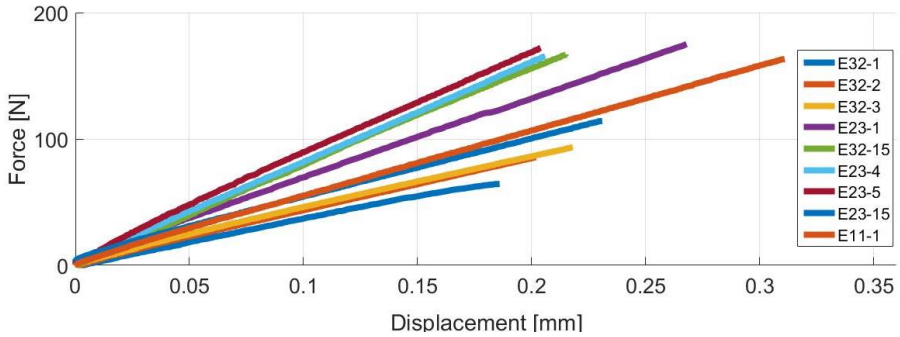

Fig. IV. Force vs displacement results of the test for the CT specimens.

After the tests have been performed, the crack length of each specimen could be measured and the mean value computed – see Table 1.

Also, the indentation tests, using 5 samples, were performed following a similar procedure and the displacement-force relationship could be obtained – see Fig. V.

Specimen	Centre pre-crack length (mm)	Side pre-crack length (mm)		Pre-crack length, a (mm)
E32-1	4.66	9.83	8.85	23.78
E32-2	7.52	5.46	8.05	23.01
E32-3	4.78	4.34	6.30	21.14
E23-1	2.08	2.55	3.67	18.77
E32-15	4.74	3.87	2.82	19.81
E23-4	2.97	3.15	2.76	18.96
E23-5	3.50	1.76	1.81	18.36
E23-15	5.05	5.80	7.13	21.99
E11-1	2.76	4.21	5.48	20.15

Table 1. Length of the pre-crack for each specimen. The pre-crack length, a, is computed as the mean value of the pre-crack at the center and the laterals.

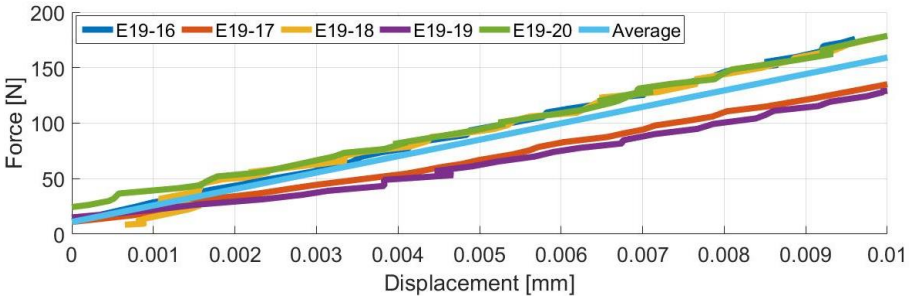

Fig. V. Force vs displacement results of the indentation test.

1) Critical Stress Intensity Factor

The critical stress intensity factor, K_{IC}, is computed from the conditional value K_Q in (1).

$$K_Q = \frac{P_Q}{B \cdot W^{1/2}} \cdot f(x) \quad [MPa \cdot m^{1/2}] \tag{1}$$

$$f(x) = ((2+x) \cdot (0.886 + 4.64 \cdot x - 13.32 \cdot x^2 + 14.72 \cdot x^3 - 5.6 \cdot x^4))/(1-x)^{\frac{3}{2}} \tag{2}$$

$$x = a/W \tag{3}$$

where: P_Q is obtained from the test record, in kN; B is the specimen thickness, in cm; W is the specimen width, in cm; a is the crack length, in cm.

2) Critical Strain Energy Release Rate

The critical strain energy release rate, G_{IC}, is computed from the conditional value G_Q in (4).

$$G_Q = \frac{U}{B \cdot W \cdot \phi} \quad [J \cdot m^2] \tag{4}$$

$$\phi = ((1.9118 + 19.118 \cdot x - 2.5122 \cdot x^2 - 23.226 \cdot x^3 + 20.54 \cdot x^4) \cdot (1-x))/((19.118 - 5.0244 \cdot x - 69.678 \cdot x^2 + 82.16 \cdot x^3) \cdot (1-x) + 2 \cdot (1.9118 + 19.118 \cdot x - 2.5122 \cdot x^2 - 23.226 \cdot x^3 + 20.54 \cdot x^4)) \tag{5}$$

$$x = a/W \tag{6}$$

$$U = \frac{1}{2} \cdot P_Q \cdot (u_Q - u_i) \tag{7}$$

where: U is the corrected energy, in J; B is the thickness, in m; W is the width, in m; ϕ is the energy-calibration factor; a is the crack length, in mm, P_Q is obtained from the test record, in kN; u_Q is the axial displacement related to P_Q in the CT test; u_i is the axial displacement related to P_Q in the indentation test.

3) Results

Table 2 shows the conditional values of the fracture parameters for each of the specimens.

Specimen	**K_Q (MPa·m$^{1/2}$)**	**G_Q (J/m^2)**
E32-1	0.82571	84.015
E32-2	0.94771	116.147
E32-3	0.75543	127.330
E23-1	0.97823	269.940
E32-15	1.10151	211.390
E23-4	0.96846	197.257
E23-5	0.92615	200.439
E23-15	1.06518	169.872
E11-1	1.15743	313.081

Table 2. Value of the fracture parameters for each specimen.

4) Verifications

To validate the results, some conditions need to be checked:

- The ratio a/W should be in the range 0.45 to 0.55 and the difference between the largest and shortest lengths of the pre-crack should be less than 10%.
- The size criteria in (8) must be met to state that $K_Q = K_{IC}$ and $G_Q = G_{IC}$. It ensures plain strain and a sufficient distance between the edge of the specimen and the tip of the pre-crack to avoid plasticity.

$$B, a, (W - a) > 2.5 \cdot (K_Q/\sigma_y)^2 \quad (8)$$

Although not all verifications could be satisfied due to the lack of accuracy on the pre-cracks, all samples met the conditions of the size criteria and therefore the mean value of the fracture parameters for the tested material could be computed (see Table 3).

	K_{IC} (MPa·m$^{1/2}$)	**G_{IC} (J/m^2)**
Mean values	0.99320	212.758

Table 3. Mean values of the fracture parameters.

B. Second Batch

The crack growth by the fatigue method was very quick and Paris' law could not be found. Although no visible damage could be observed prior to fracture of the specimen, beach marks could be distinguished on the fracture surface of the CT specimen, as Fig. VI shows.

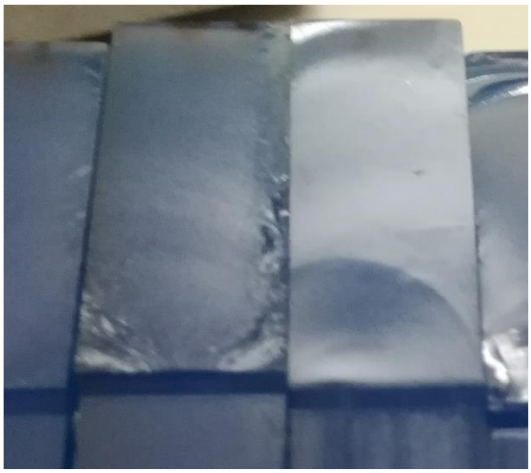

Fig. VI. Beach marks on the specimens pre-cracked by fatigue.

C. Third Batch

The clamp surface to apply the compressive load was a rectangle of sides 22x10 mm. In **Error! Reference source not found.**, the compression and tension loads applied to the specimens are shown. Also, the case of failure as illustrated in Fig. III is indicated.

Specimen	Compression (N)	Tension, P (N)	Case
E32-6	833.33	834	
	1083.33	1300	
	1083.33	715	A
E32-7	1083.33	1000	
	1083.33	1300	C
E32-8	1083.33	1150	
	1083.33	1072	C
E32-9	1083.33	1482	C
E32-12	1083.33	1047	A
E32-13	1667.67	1381	C

Table 4. Loads applied to the specimens pre-cracked by the new method and mode of growth of the pre-crack.

The behavior of this material for this pre-cracking method was different for each specimen and therefore, a general conclusion could not be obtained. Moreover, for E32-6 and E32-7, a creep behavior, which was not expected for this material, was observed.

IV. NUMERICAL SIMULATION

Two different models were simulated. The 2D model was used to simulate the test indicated in the standard and the 3D one was necessary to verify the new method for pre-cracking.

A. Models

1) Two-Dimensional Model

The specimen's material was simulated as an elastic, isotropic material with Poisson's ratio equal to 0.36 and a Young's modulus of 2000 MPa (approximately, determined from simulations and experimental results). The section was defined as a homogeneous solid subjected to plane strain through its thickness. The model in Fig. VII was partitioned such that the mesh at the crack tip, which is the area of interest, is finer and in a spider web configuration in that region.. The loading and boundary conditions were applied similarly as in the experimental test: the loading was applied on the upper hole, where the x-displacement was restricted and on the lower hole, the x- and y-displacements were restricted. The rotation around the z-axis is free in both holes.

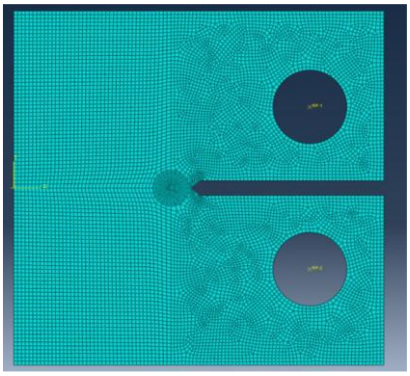

Fig. VII. 2D model of the CT sample.

2) Three-Dimensional Model

Using the same material specifications, the 3D model was created as a deformable solid. This model, which can be seen in Fig. VIII, is partitioned as the 2D model and includes another division to apply a compression load to limit the growth of the pre-crack. The boundary conditions restrict the displacement around the x- and z- axes and the rotation around the x- and y- axes in the upper hole and in the lower hole, all the degrees of freedom are restricted but the rotation around the z-axis.

B. Analyses

1) Critical Stress Intensity Factor and Critical Strain Energy Release Rate

A numerical simulation to obtain the fractures parameters for each pre-crack length was performed. Each specimen was loaded with the respective fracture load from the experimental tests. Table 4 shows the results of the numerical fracture parameters.

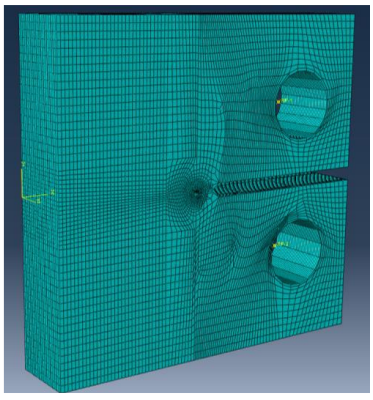

Fig. VIII. 3D model of the CT sample.

Specimen	K_{IC} (MPa·m$^{1/2}$)	G_{IC} (J/m^2)
E32-1	0.42252	81.146
E32-2	0.52182	123.769
E32-3	0.48498	106.921
E23-1	0.75968	262.323
E32-15	0.78196	277.933
E23-4	0.72699	240.234
E23-5	0.72483	238.808
E23-15	0.63764	184.809
E11-1	0.78403	279.407

Table 4. Value of the fracture parameters for each specimen calculated on Abaqus.

2) Crack Length – Stress Intensity Factor Relationship

Using the 2D model, also a relationship between the crack length a and the stress intensity K_I was studied. Each crack length was simulated with different loads. In Fig. IX, it can be seen that K_I increases as a increases and that it is proportional to the load as (1) states.

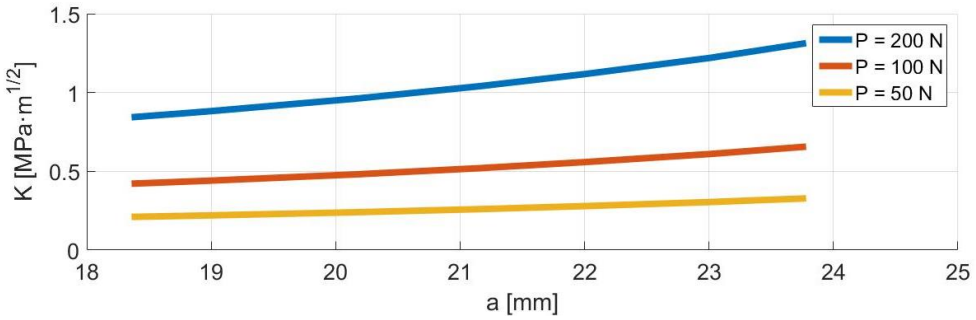

Fig. IX. Pre-crack length vs K_I for different values of the axial load.

3) Crack Length – Load Relationship

To verify the new method for pre-cracking, also the 3D model was used since a transversal force is applied.

The stress intensity factor was analyzed for the following loadings: pure tension - a loading of 200 N on the upper hole-, pure compression - a load of 1000 N on the rectangular surface - and mixed tension-compression - the combination of both loadings. This loading doesn't correspond to the fracture mode I, but K_{II} and K_{III} could be neglected.

Fig. X shows the evolution of the stress intensity factor in mode I, K_I, as the load is increased – in yellow for the 3D model and in blue for the 2D model.

A linear progression is observed in both models, but there is a slight difference in their slopes, which lead to a value of K_I=0.8677 MPa·m$^{1/2}$ for the 2D model and K_I=0.9666 MPa·m$^{1/2}$ for the 3D model.

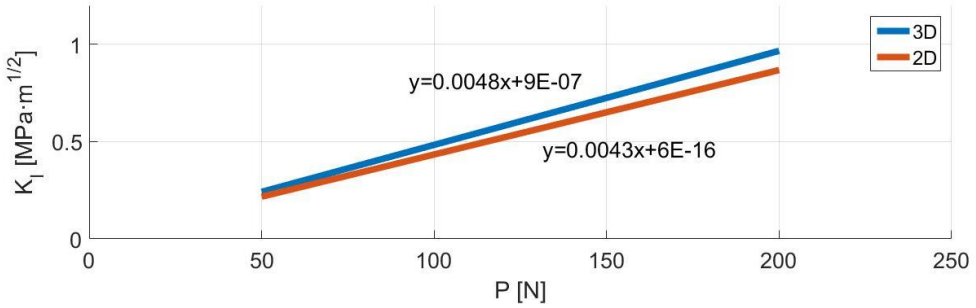

Fig. X. K_I vs tension load of the 2D and 3D model at the centerpoint of the thickness.

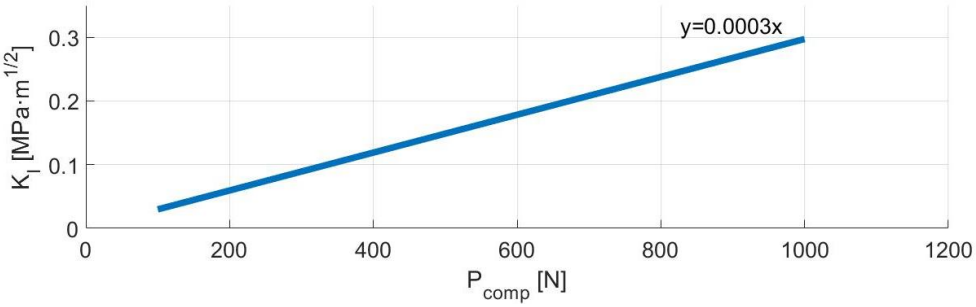

Fig. XI. K_I vs compression load at the centerpoint of the thickness of the CT specimen.

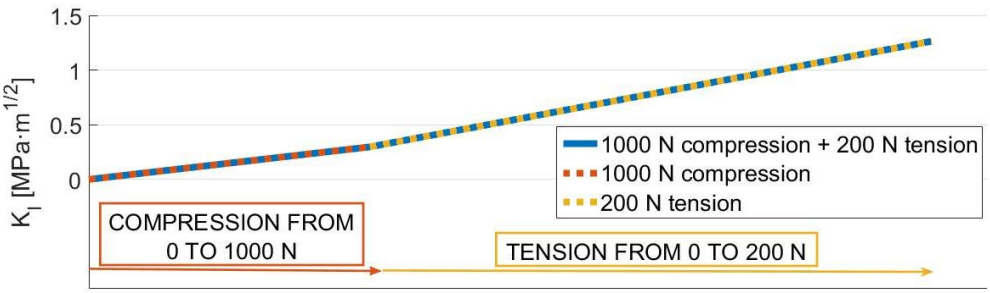

Fig. XII. K_I value for variation of the load.

Fig. XI shows the influence on K_I of the transversal compression load. The slope is 10 times smaller and when the compression load is 1000 N, the stress intensity factor is K_I=0.7432 MPa·m$^{1/2}$. Combining both loadings, the graph in Fig. XII is obtained, showing that the principle of superposition holds.

The Von Mises stress distribution was analyzed for five loading cases: pure tension in plane strain state, pure tension, pure compression, mixed compression and tension and pure tension in plane stress state. Results are shown in Fig. XIII, in which the characteristic plastic zone in plane stress and plane strain can be recognized. [5]

Loading	Crack tip	Crack front	K_I (MPa·m$^{1/2}$)
Tension plane strain	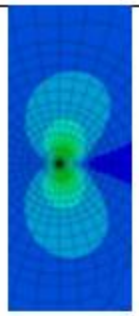	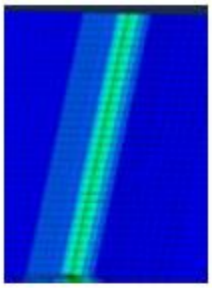	0.87689
Tension	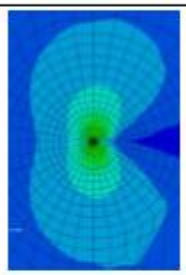	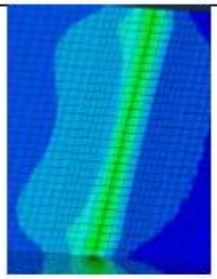	0.96655
Compression	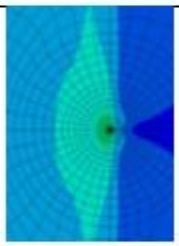	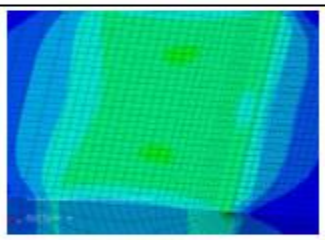	0.29730
Compression + Tension	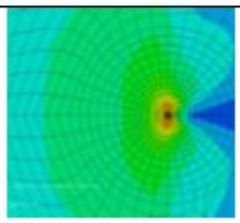	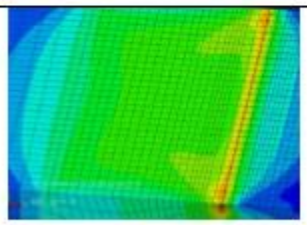	1.26385
Tension plane stress	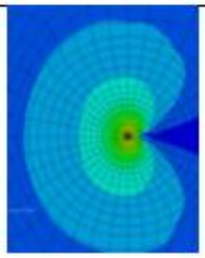	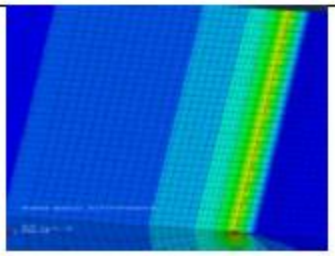	0.87502

Fig. XIII. Plastic zone size and shape for different loadings of the CT model.

Besides the notable increase of the plastic zone size from the plane strain state to the plane stress state, which can be explained as a consequence of the loss of constraint in the crack surroundings, it can be also observed that the compression load contributes to the increase of the plastic zone size. This means a higher failure load could be expected when the convenient loads are applied.

V. DISCUSSION OF RESULTS

As Table 5 shows, there are great error percentages between the experimental fracture parameters and the numerically simulated ones. This could be due to the inaccuracy of the pre-crack in the experimental tests and to the differences between the specimens and the models used for the simulation. It must be noted that not all the verifications could be held because of the difficult task of creating the pre-cracks and that the shape of the pre-cracks is very different in the specimens and in Abaqus, in which it is simulated as a straight line.

	KIC ($MPa \cdot m^{1/2}$)	**KIC Abaqus ($MPa \cdot m^{1/2}$)**	**Error (%)**
Specimen	0.99320	0.70002	29.46
Average	**G_{IC} (J/m^2)**	**GIC Abaqus (J/m^2)**	**Error (%)**
	212.758	227.205	15.83

Table 5. Table for the comparison of the experimental and numerical results of the fracture parameters.

VI. CONCLUSIONS

The epoxy resin EPOLAM 2025 was characterized by its fracture parameters using CT specimens as the ASTM D5045 standard states. Due to the difficulty to create the pre-cracks and the consequent inaccuracy, the values K_{IC}=0.99320 $MPa \cdot m^{1/2}$ and G_{IC}=212.758 J/m^2 may not be very precise.

These fracture parameters were also calculated with the finite element Abaqus code. The results were K_{IC}=0.70002 $MPa \cdot m^{1/2}$ and G_{IC}=227.205 J/m^2. The difference with respect to the experimental results may be due to the lack of resemblance between the pre-crack shapes of the specimens and the models.

Out of the alternative methods for pre-cracking, the fatigue method was not suitable for this brittle polymeric material. Instead, although the method that consists in applying a transversal force while a tension load is being applied could not be implemented in the experimental section, it could be justified with numerical analysis.

The Von Mises stress distribution analysis demonstrated that the lateral compression load has presumably improved the failure conditions of the specimen because it increases the plastic zone size around the pre-crack's tip.

ACKNOWLEDGMENT

The authors are thankful for the financial support of the research project Ref. DPI2016-80389-C2-2-R from the Spanish Ministry of Economy and Competitiveness.

REFERENCES

[1] Álvarez Vázquez, A.; F. Pelayo; Fernández-Canteli, A.; Lamela, M.J.; Martinho, A.; McKenna, J.; Muñiz-Calvente, M.; Pintado, J.M.; Salazar, A. Metodología para la caracterización probabilística de polímeros.

[2] *ASTM D5045-99, Standard Test Methods for Plane-Strain Fracture Toughness and Strain Energy Release Rate of Plastic Materials.* West Conshohocken, PA: ASTM International, 1999, www.astm.org. <http://www.astm.org/cgi-bin/resolver.cgi?D5045>

[3] Kuppusamy, Nithiananthan. Tomlinson, Rachel A. "Repeatable pre-cracking preparation for fracture testing of polymeric materials". *Engineering Fracture Mechanics*. Volume 152. February 2016, Pages 81-87. <https://doi.org/10.1016/j.engfracmech.2015.12.007>.

[4] Cardoso Martinho, André. *Probabilistic Characterization of Epoxy Adhesives*. Master Thesis, Universidade do Porto, 2018.

[5] Anderson, T.L. *Fracture Mechanics. Fundamentals and Applications.* 3rd edition. Boca Raton, FL: CRC Press, 2005.